Neuropathology and Applied Neurobiology (2014), **40**, 489–501 doi: 10.1111/nan.12056

Phosphatidylinositol-4,5-bisphosphate is enriched in granulovacuolar degeneration bodies and neurofibrillary tangles

T. Nishikawa*, T. Takahashi*, M. Nakamori*, Y. Yamazaki†, T. Kurashige*, Y. Nagano*, Y. Nishida‡, Y. Izumi§ and M. Matsumoto*

**Department of Clinical Neuroscience and Therapeutics, Hiroshima University Graduate School of Biomedical and Health Sciences, †Department of Neurology, Hiroshima Prefectural Hospital, Hiroshima, ‡Department of Neurology, Itsuki Hospital, and §Department of Neurology, Tokushima University, Tokushima, Japan*

T. Nishikawa, T. Takahashi, M. Nakamori, Y. Yamazaki, T. Kurashige, Y. Nagano, Y. Nishida, Y. Izumi and M. Matsumoto (2014) *Neuropathology and Applied Neurobiology* **40**, 489–501
Phosphatidylinositol-4,5-bisphosphate is enriched in granulovacuolar degeneration bodies and neurofibrillary tangles

Aims: Among the pathological findings in Alzheimer's disease (AD), the temporal and spatial profiles of granulovacuolar degeneration (GVD) bodies are characteristic in that they seem to be related to those of neurofibrillary tangles (NFTs), suggesting a common mechanism underlying the pathogenesis of these structures. Flotillin-1, a marker of lipid rafts, accumulates in lysosomes of tangle-bearing neurones in AD patients. In addition, recent reports have shown that GVD bodies accumulate at the nexus of the autophagic and endocytic pathways. The aim of this study was to elucidate the distribution of the lipid component of lipid rafts, phosphatidylinositol-4,5-bisphosphate [PtdIns(4,5)P2], in AD and other neurodegenerative disorders. **Methods:** We compared PtdIns(4,5)P2 immunoreactivity in the hippocampus, entorhinal cortex and neocortex of five AD cases, 17 cases of other neurodegenerative disorders and four controls. In addition, we performed double staining using markers of GVD, NFTs and lipid rafts for further characterization. **Results:** Immunohistochemical analysis revealed that PtdIns(4,5)P2 was selectively enriched in GVD bodies and NFTs. Although immunoreactivity for PtdIns(4,5)P2 was also evident in NFTs composed of hyperphosphorylated tau, PtdIns(4,5)P2 was segregated from phosphorylated tau within NFTs by double immunofluorescence staining. In contrast, PtdIns(4,5)P2 colocalized with the lipid raft markers flotillin-1 and annexin 2, within GVD bodies and NFTs. **Conclusions:** These results suggest that lipid raft components including PtdIns(4,5)P2 play a role in the formation of both GVD bodies and NFTs.

Keywords: Alzheimer's disease, granulovacuolar degeneration, lipid raft, neurofibrillary tangle, phosphatidylinositol-4,5-bisphosphate

Introduction

Alzheimer's disease (AD) is pathologically characterized by the presence of senile plaques, polymorphous amyloid beta protein deposits and neurofibrillary tangles (NFTs) composed of hyperphosphorylated tau. NFTs but not senile plaques are pathological hallmarks of a diverse array of neurodegenerative disorders other than AD, named tauopathies, such as progressive supranuclear palsy, corticobasal degeneration, and Pick's disease. In the hippocampi of tauopathy patients, granulovacuolar degeneration (GVD) bodies occur concomitantly with NFTs. GVD results in the formation of basophilic small

Correspondence: Tetsuya Takahashi, 1-2-3 Kasumi, Minami-ku, Hiroshima 734-8551, Japan. Tel: +81 82 257 5201; Fax: +81 82 505 0490; E-mail: tetakaha@mac.com

inclusions in the perinuclear region of pyramidal neurones, comprising 3- to 5-μm-diameter spherical vacuoles surrounded by a halo-like clear zone. In addition to TDP-43, phosphorylated Smad2/3 (pSmad2/3), charged multivesicular body protein 2B (CHMP2B), several tau kinases including glycogen synthase kinase (GSK)-3β and cyclin-dependent kinase 5 (CDK5) also exist in GVD bodies implying that GVD bodies might be a site of tau modification that results in the formation of NFTs [1–5]. In pyramidal neurones, CDK5 immunoreactivity is found not only in GVD bodies, but also within NFTs as fine granules [5]. In accordance with the granules reported by Girardot *et al.*, these CDK5-positive fine granules are spherical, stained homogenously, and of a similar size to intraluminal vesicles of GVD bodies, resembling the granules immunostained for the genuine raft protein flotillin-1 [6].

Recently, it was reported that GSK-3β and CDK5 are recruited to neuronal lipid raft microdomains upon stimulation [7,8]. Lipid rafts, specialized plasma membrane domains, provide a platform for cell signalling [9]. Recent reports have also emphasized the importance of lipid rafts in the biogenesis and accumulation of amyloid protein implying that lipid rafts play a role in the pathogenesis of AD [10–13]. These lines of evidence suggest that CDK5-positive GVD bodies might be derived from lipid rafts.

Little is known about the lipid composition of GVD bodies or vesicles associated with NFTs [14]. Although cholesterol and sphingolipids are the major component of lipid rafts, phosphatidylinositol 4,5-bisphosphate [PtdIns(4,5)P2] is also a component of lipid rafts in the cell membrane [15], and is important for many aspects of membrane trafficking in neurones [16]. We hypothesized that lipid rafts are involved in the pathological mechanism underlying AD. Thus, in the present study, we investigated the distribution of specific phosphoinositides in the brains of AD patients and patients with other neurodegenerative diseases.

Materials and methods

Subjects

Five cases of AD [mean age = 74.2 years ± 6.18 standard error of the mean (SEM)], three cases of myotonic dystrophy (MyD), six cases of amyotrophic lateral sclerosis (ALS), two cases each of Parkinson's disease with dementia (PDD) and multiple system atrophy (MSA), and one case each of corticobasal degeneration (CBD), progressive supranuclear palsy (PSP), Pick's disease (PiD), and pantothenate kinase-associated neurodegeneration (PKAN) [non-AD neurodegenerative disease; mean age = 67.8 years ± 8.86 SEM], and four control cases (without neurodegenerative disorders according to clinical history and confirmed by neuropathological examination [mean age = 64.0 years ± 11.6 SEM]) were selected. The clinical profiles, GVD stages [17], phases of amyloid beta protein deposition phases [18], Braak NFT stages [19], frequencies of neuritic plaques according to the method of The Consortium to Establish a Registry for Alzheimer's Disease [20], and degrees of AD neuropathologic change [21] of these patients are shown in Table 1. The use of human materials conformed to the ethical guidelines of Hiroshima University Graduate School of Biomedical and Health Sciences, Hiroshima, Japan. All AD cases fulfilled the quantitative neuropathological criteria for diagnosis of AD according to the National Institute on Aging-Alzheimer's Association (NIA-AA) guidelines for the neuropathologic assessment of AD; that is, Alzheimer Disease Neuropathologic Change scores of A3, B3 or C3 [21]. All MyD cases were compatible with clinical features, and the numbers of CTG repeats in the myotonin protein kinase gene were all >3000.

Brain tissue

Autopsies were performed within 24 h of death. Brains and spinal cords were fixed in 10% (v/v) formalin for 3 weeks, and 7-μm thick paraffin-embedded sections were prepared for subsequent procedures. We sampled and analysed the medial temporal lobe, including the hippocampus and neocortex, of all cases for GVD bodies and NFTs, and the brain stem and spinal cord tissues of non-tauopathy cases, such as PDD, MSA, ALS and control cases, for Lewy bodies and Bunina bodies.

Immunohistochemistry

The antibodies used for immunohistochemistry and immunofluorescence studies are listed in Table 2. The sections were deparaffinized and rehydrated. For antigen retrieval, microwave treatment in distilled water for 10 min was performed, followed by washing in phosphate-buffered saline (PBS) for 3 min. Deparaffinized sections were then incubated with 3% H_2O_2 in PBS for 60 min to eliminate endogenous peroxidase activity in tissues. Each section was incubated with primary antibodies overnight at 4°C. The sections were then washed three times in PBS

Table 1. Subject characteristics

Case No.	*Diagnosis*	*Gender*	*Age*	*GVD stage*	*Aβ phase*	*NFT stage*	*CERAD*	*AD neuropathologic change*
1	AD	M	73	5	5	6	Frequent	High
2	AD	F	66	5	5	6	Frequent	High
3	AD	F	75	5	5	6	Frequent	High
4	AD	F	85	5	5	5	Frequent	High
5	AD	F	72	5	5	5	Frequent	High
6	MyD	M	57	4	3	2	Sparse	Low
7	MyD	F	59	1	2	2	Sparse	Low
8	MyD	M	48	1	3	1	Sparse	Low
9	CBD	F	75	2	3	3	Frequent	Intermediate
10	PSP	F	71	2	1	2	Sparse	Low
11	PiD	M	66	1	0	3	None	Not
12	PKAN	F	57	5	1	5	Sparse	Low
13	PDD	M	86	1	4	2	Frequent	Low
14	PDD	M	75	1	4	2	Frequent	Low
15	MSA	F	73	1	5	2	Moderate	Low
16	MSA	F	72	1	3	2	Frequent	Low
17	ALS	F	70	1	1	2	Moderate	Low
18	ALS	F	67	0	3	1	Sparse	Low
19	ALS	M	77	0	3	0	Frequent	Low
20	ALS	M	63	0	2	0	Sparse	Low
21	ALS	M	65	0	0	0	None	Not
22	ALS	F	72	0	5	0	Frequent	Low
23	CON	F	49	0	0	0	None	Not
24	CON	F	58	0	0	0	None	Not
25	CON	F	69	0	0	0	None	Not
26	CON	M	80	0	0	0	None	Not

CON, control case; AD, Alzheimer's disease case; MyD, myotonic dystrophy case; CBD, corticobasal degeneration case; PSP, progressive supranuclear palsy case; PiD, Pick's disease case; PKAN, pantothenate-kinase-associated neurodegeneration case; PDD, Parkinson's disease with dementia case; MSA, multiple system atrophy case; ALS, amyotrophic lateral sclerosis case; F, female; M, male; Age, age at death.

Table 2. List of primary antibodies

Antigen	*Clone*	*Isotype*	*Source*	*Animal*	*Dilution*
PtdIns(4,5)P2	Monoclonal (2C11)	IgM	Santa Cruz	Mouse	1:2000
Annexin2	Polyclonal	IgG	Epitomics	Rabbit	1:100
CHMP2B	Polyclonal	IgG	Abcam	Rabbit	1:600
CDK5	Polyclonal (C-8)	IgG	Santa Cruz	Rabbit	1:200
Flotillin-1	Monoclonal	IgG	BD bioscience	Mouse	1:200
p-tau	Monoclonal (AT8)	IgG	Innogenetics	Mouse	1:800

and incubated with horseradish peroxidase (HRP)-conjugated anti-mouse antibody or anti-rabbit antibody for 30 min at room temperature. The avidin–biotin complex method was used to detect the mouse monoclonal IgM-type antibody anti-PtdIns(4,5)P2 (clone 2C11). The sections were then washed three times in PBS and incubated at room temperature with 3, 3-diaminobenzidine (Dako, Glostrup, Denmark).

We also performed haematoxylin and eosin (H&E) staining. After observing GVD bodies and NFTs in the hippocampus, we destained sections in absolute ethanol, and then processed them for PtdIns(4,5)P2 immunohistochemical analysis using the antibody 2C11. As controls, we prepared stained sections without primary antibody. In addition, we performed control experiments in which we blocked the immunogenicity of PtdIns(4,5)P2 with 10 mM neomycin sulphate/PBS prior to immunohistochemical staining with 2C11.

We also performed labelling of PtdIns(4,5)P2 using PLCδ_1PH-GST on brain sections according to Watt *et al.*

[22]. Briefly, sections were incubated in PBS for 10 min, PBS containing 0.2% Triton X-100, 3% fatty acid-free bovine serum albumin for 20 min and then with droplets of PLCδ_1PH–GST (5 μg/ml) in PBS containing 0.2% Triton X-100, 3% bovine serum albumin for 2 h. Following washes in PBS, the GST was visualized using HRP conjugated anti-GST antibodies.

Immunofluorescence staining

We performed double staining on sections, including sections from the hippocampus and the parahippocampal gyrus, for further characterization. First, paraffin-embedded sections were irradiated with UV light overnight at 4°C to reduce autofluorescence by photobleaching tissue sections. After irradiation, we applied the same primary antibodies as described above. Some of these primary antibodies were detected using the following secondary antibodies (dilution 1:1000; Molecular Probes, Eugene, OR, USA): Alexa Fluor 488 donkey anti-mouse IgM and Alexa Fluor 548 donkey anti-rabbit IgG. The others were detected using the tyramide signal amplification (TSA) method with the same HRP-conjugated secondary antibodies as described above together with TSA™KIT #12: Alexa Fluor 488 donkey and TSA™ KIT#4: Alexa Fluor 568 donkey (Invitrogen™, Eugene, OR, USA). The slides were mounted with Vectashield (Vector Laboratories, Burlingame, CA, USA) and observed under an LSM510 confocal laser scanning microscope (Carl Zeiss AG, Oberkochen, Germany).

Moreover, we prepared 20-μm-thick paraffin-embedded sections and stained them using immunofluorescence techniques with 2C11 as primary antibody and Alexa Fluor 488 donkey anti-mouse IgM as secondary antibody for the construction of 3-dimensional images using an FV1000D confocal laser scanning microscope (Olympus, Tokyo, Japan).

Results

PtdIns(4,5)P2 is a selective marker for both GVD bodies and NFTs

In the brains of AD cases, PtdIns(4,5)P2-positive structures were observed mainly in the hippocampal neurones. This staining pattern was reminiscent of those for GVD bodies and NFTs, appearing as accumulations of fine granules (Figures 1 and 2). We classified the PtdIns(4,5)P2-positive cells in AD brains into three categories based on the structures they contained, as follows: GVD bodies, NFTs and 'GVD bodies + NFTs'. We reconstituted 3-dimensional images using confocal laser scanning microscopy (Figure 3) and confirmed that these structures were consistent with GVD bodies and NFTs. The structures were immunopositive for PtdIns(4,5)P2 up to an antibody dilution of 1:8000, but were only faintly stained when the antibody was diluted to a ratio of 1:16 000. In other tauopathy cases such as MyD, CBD, PSP, PiD and PKAN, PtdIns(4,5)P2-positive structures were also observed in the hippocampal neurones, although they were fewer in number than they were in AD cases. In non-tauopathy cases such as PDD, MSA, ALS and control cases, PtdIns(4,5)P2-positive structures were observed only scarcely. In addition, we examined the brain stem and the spinal cord tissues of non-tauopathy cases and found no specific staining suggestive of Lewy bodies and no Bunina bodies, small eosinophilic neuronal inclusions commonly seen in patients with ALS, immunopositive for PtdIns(4,5)P2 (data not shown).

The specificity of 2C11

The specificity of the anti-PtdIns(4,5)P2 antibody (clone 2C11) used in this study has been already reported; pre-incubation of the 2C11 antibody with an excess of liposomes containing different phosphoinositides showed that the specific staining was abolished by PtdIns(4,5)P2, but not by any other lipid, including PtdIns(3,4,5)P3, PtdIns(4,5)P2, PtdIns(3,4)P2 and PtdIns(3,5)P2 [23,24]. Another study showed that binding of 2C11 was effectively prevented by incubation with neomycin, an aminoglycoside antibiotic that binds with high affinity to several phosphoinositides including PtdIns(4,5)P2, and that incubation with a GST-tagged PH domain of PLCδ_1, which binds PtdIns(4,5)P2 with exquisite specificity, also reduced the intensity of staining by the 2C11 antibody [25]. We applied a GST-tagged PH domain of PLCδ_1 directly onto tissue sections and visualized it using an HRP-conjugated anti-GST antibody. The staining pattern obtained by this method was essentially identical to that following immunohistochemistry using the 2C11 antibody (Figure 1**p**–**r**). We also investigated the specificity of 2C11 for PtdIns(4,5)P2 using neomycin, a selective blocker of PtdIns(4,5)P2, and confirmed a lack of staining compared with positive controls (Figure 2**f**). Furthermore, the presence of the PtdIns(4,5)P2-binding protein

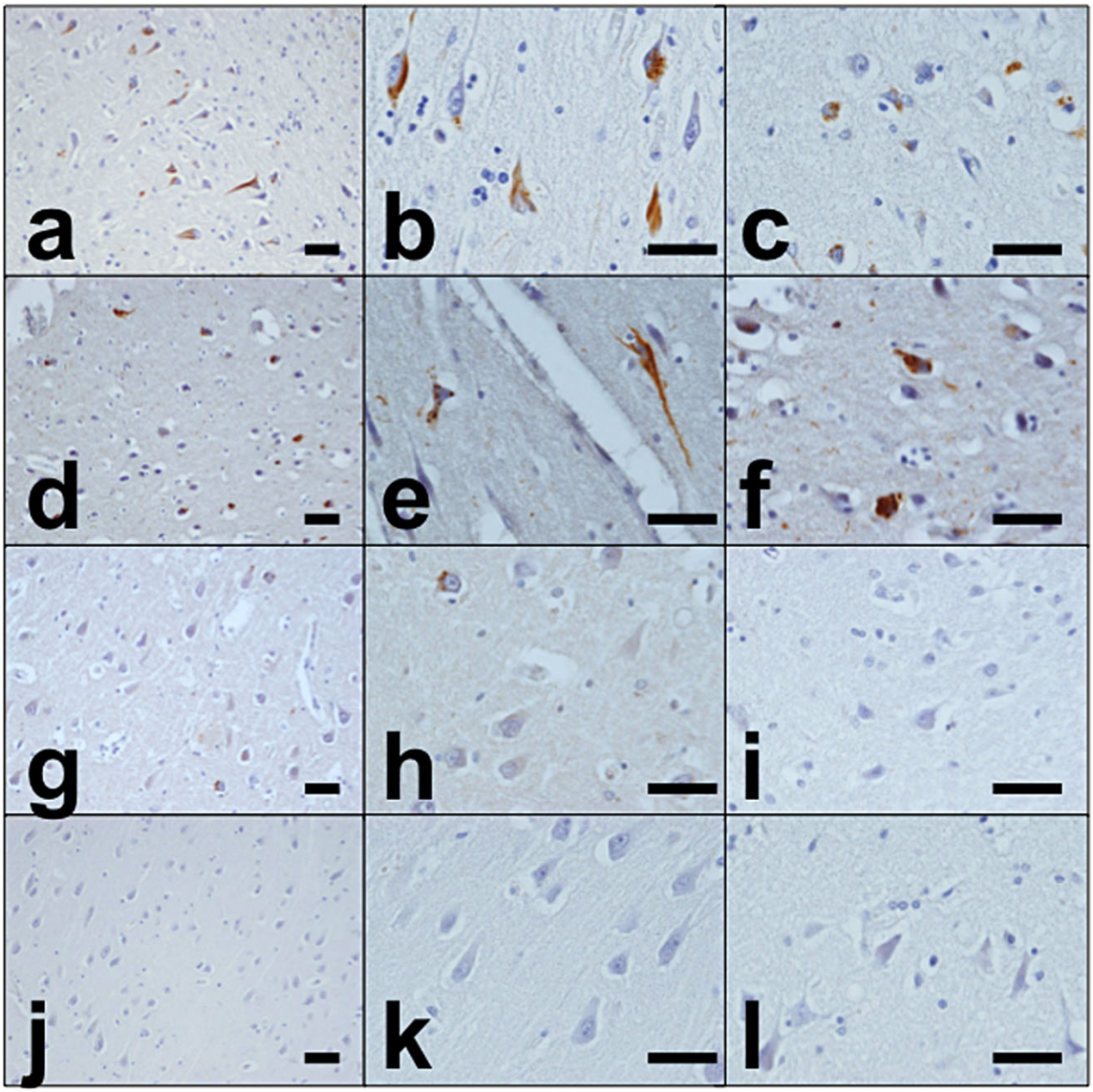

Figure 1. Immunohistochemistry for PtdIns(4,5)P2. Immunohistochemistry in AD, MyD, ALS and control cases. AD case (case 1): low-power fields in hippocampus (**a**,**b**) and neocortex (**c**). MyD case (case 6): low-power fields in hippocampus (**d**,**e**) and neocortex (**f**). ALS case (case 17): low-power fields in hippocampus (**g**,**h**) and neocortex (**i**). Control case (case 26): low-power fields in hippocampus (**j**,**k**) and neocortex (**l**). AD case (case 5): some of the detected structures are (**m**) GVD bodies, (**n**) 'GVD bodies + NFTs', and (**o**) NFTs. The specificity of immunoreactivity for PtdIns(4,5)P2 was verified using PLCδ_1PH-GST on sections, which showed essentially the same staining pattern as the anti-PtdIns(4,5)P2 antibody (**p**–**r**). Scale bars: (**a**–**l**) 50 μm, (**m**–**r**) 20 μm.

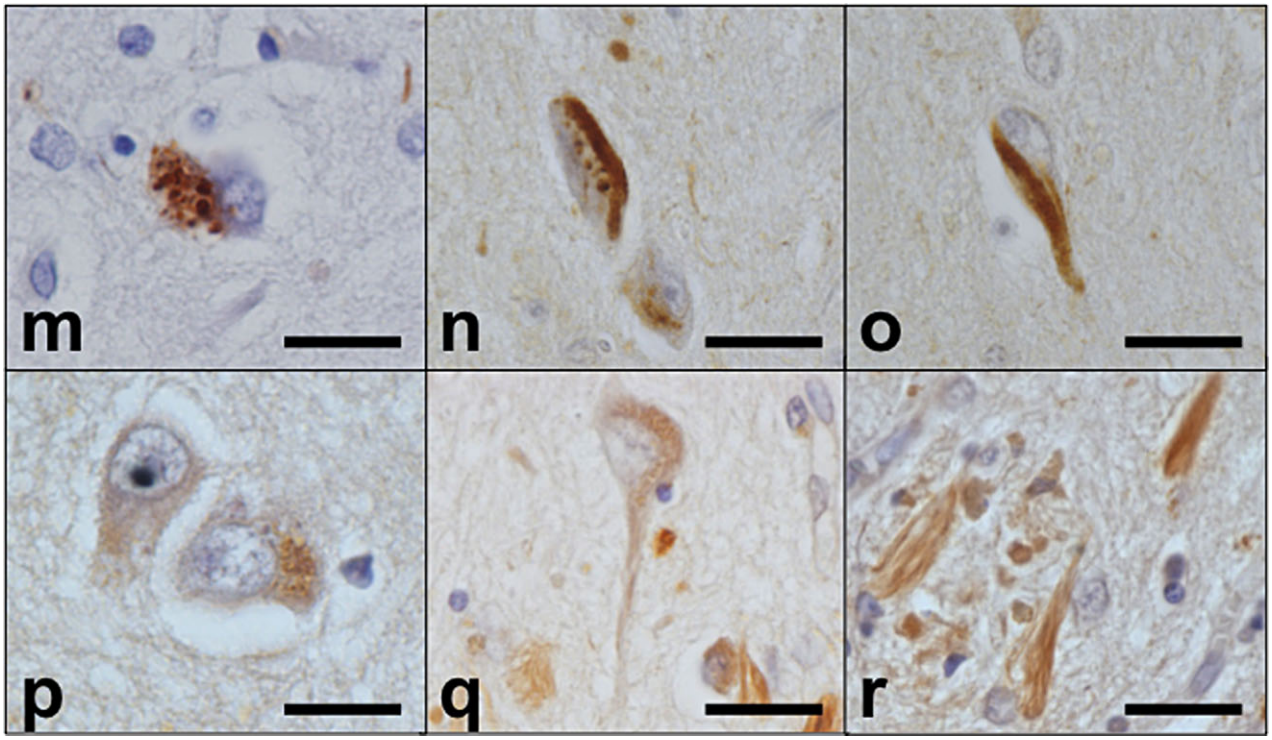

Figure 1. (*Continued*)

annexin 2 in GVD bodies and NFTs substantiates the specificity of the antibody. Taken together, our data suggested that PtdIns(4,5)P2 was specifically stained with the 2C11 antibody.

PtdIns(4,5)P2-positive structures identified by double immunofluorescence staining

We performed double immunofluorescence staining for PtdIns(4,5)P2 and several established markers to characterize the PtdIns(4,5)P2-positive structures in AD cases. First we used anti-PtdIns(4,5)P2 antibody together with an anti-CHMP2B antibody as a GVD body marker, which revealed that some of the PtdIns(4,5)P2-immunopositive granules colocalized with CHMP2B (Figure 4**a**). This result suggested that at least some PtdIns(4,5)P2-positive granules correspond to the intraluminal granules associated with GVD bodies.

Next, we used anti-PtdIns(4,5)P2 antibody together with AT8 antibody as a NFT marker, which revealed that most NFTs were immunopositive for PtdIns(4,5)P2 (Figure 4**b**). However, PtdIns(4,5)P2 and phosphorylated tau immunoreactivity patterns were not merged completely within each NFT, which means that while NFTs contain PtdIns(4,5)P2, it is segregated from AT8. The NFTs themselves showed accumulations of fine spherical granules and some granules were distributed diffusely within pyramidal neurones.

To identify the fine spherical granules, we performed double immunofluorescence staining using anti-PtdIns(4,5)P2 antibody and an anti-CDK5 antibody, which showed the colocalization on GVD bodies and fine granules, some of them in NFTs (Figure 4**c**,**d**). It has been reported that fine spherical granules as well as GVD bodies and NFTs are all immunopositive for CDK5 [5]. To investigate whether these granules are related to lipid rafts we performed double immunofluorescence staining using anti-PtdIns(4,5)P2 antibody, anti-flotillin-1 antibody and anti-annexin 2 antibody, established raft-related proteins. This revealed the colocalization of PtdIns(4,5)P2 and lipid raft-related proteins in these fine spherical granules as well as in NFTs and GVD bodies (Figure 4**e**–**h**).

Discussion

In this study, we found that PtdIns(4,5)P2 is selectively enriched in both GVD bodies and NFTs. Based on a limited dilution analysis, the anti PtdIns(4,5)P2 antibody used

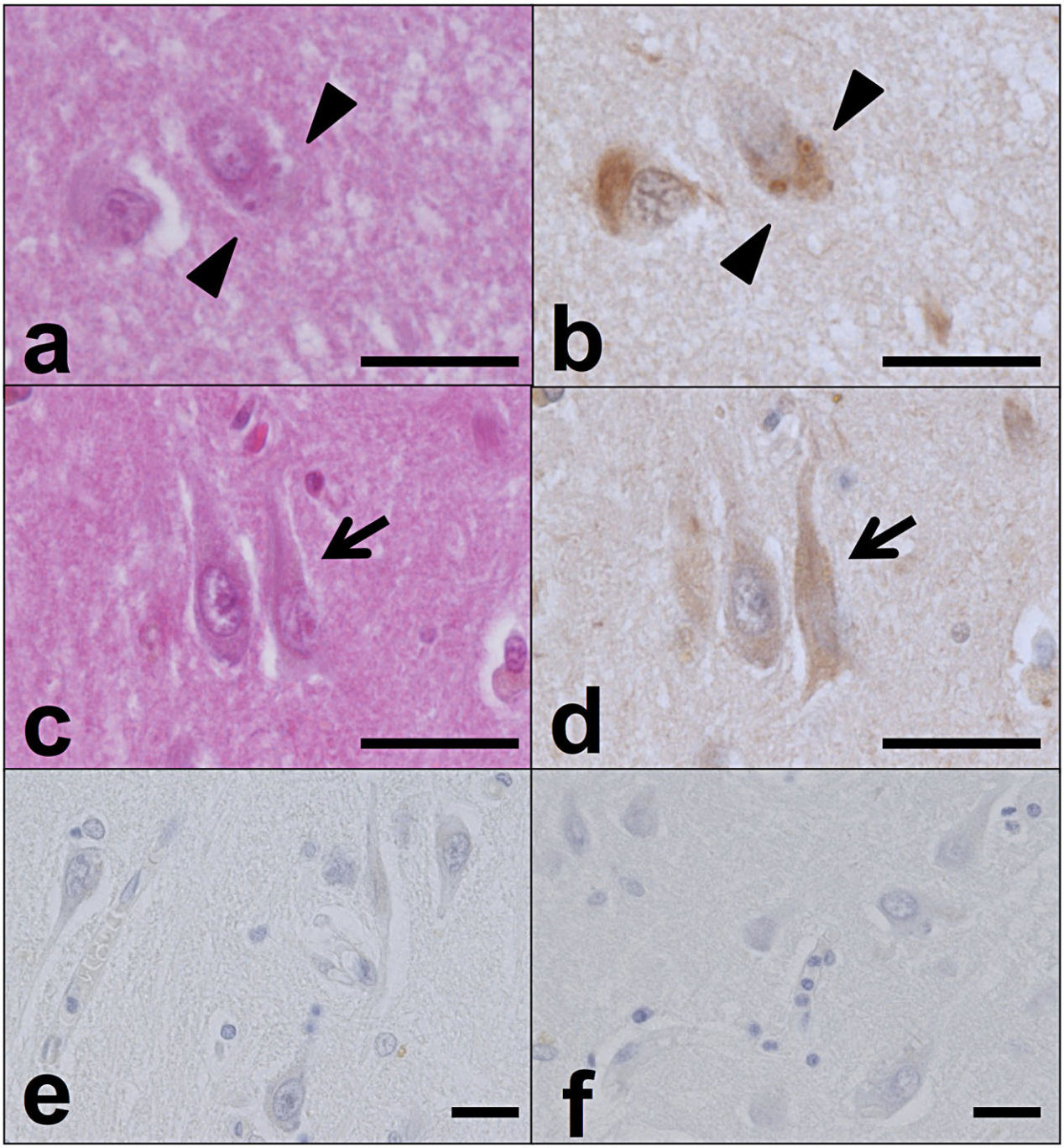

Figure 2. PtdIns(4,5)P2-positive structures corresponding to GVD bodies and NFTs. In the hippocampus of an AD case, the cellular localization of PtdIns(4,5)P2 was compared among haematoxylin and eosin (H&E)–stained sections (**a**,**c**), sections subjected to immunohistochemical analysis with 2C11 [**b**,**d**; some of the structures are GVD bodies (arrowhead) and some are NFTs (arrow)], sections incubated without primary antibody (**e**), and sections incubated with 10 mM neomycin sulphate/PBS prior to immunohistochemical staining with 2C11 (**f**). Scale bars: 20 μm.

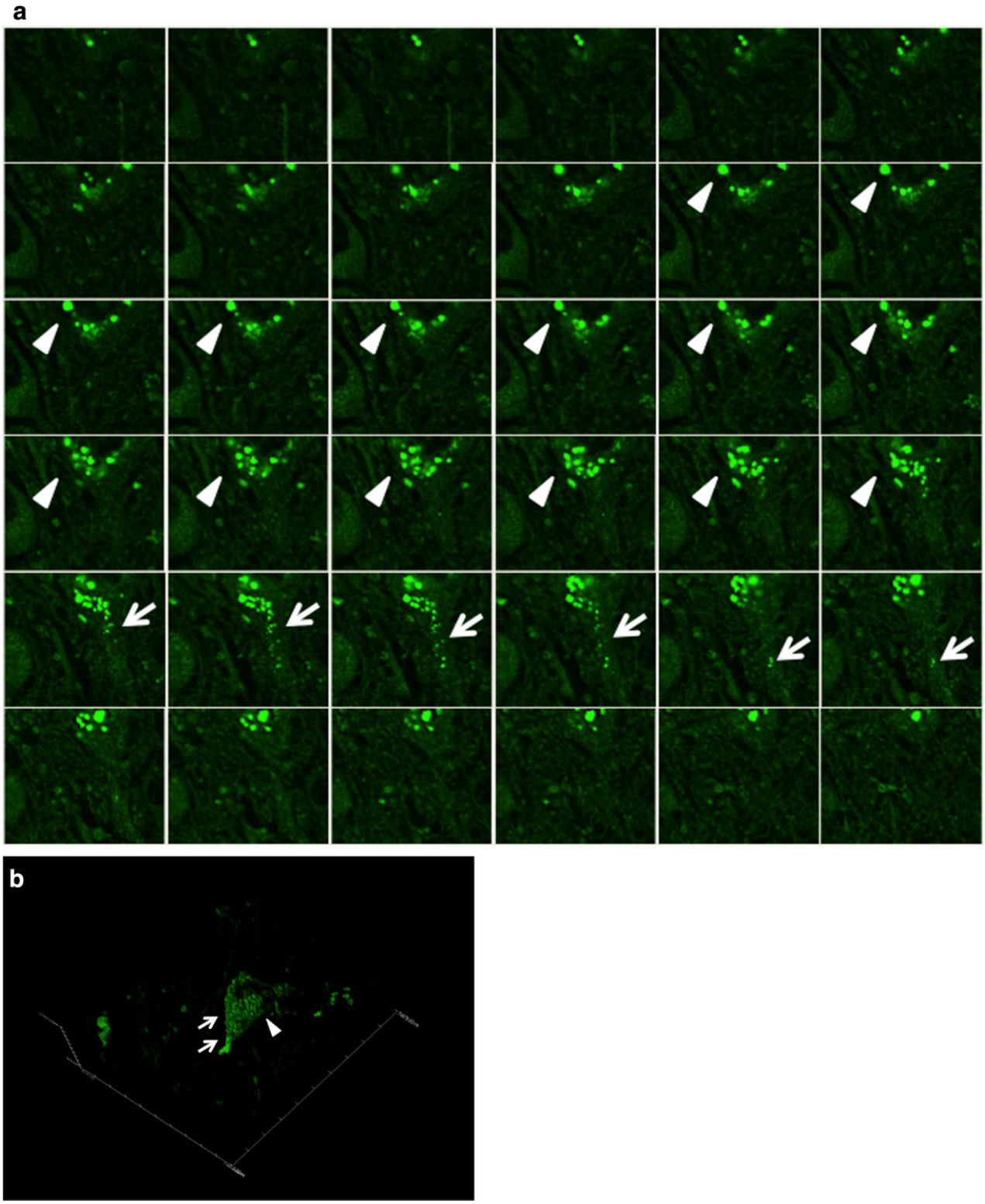

Figure 3. Three-dimensional image of PtdIns(4,5)P2-positive structures in the hippocampus. PtdIns(4,5)P2-immunopositive structures in the hippocampus in an AD case (case 1). (**a**) 2-dimensional serial images and (**b**) reconstituted 3-dimensional image. Some of the structures are GVD bodies (arrowhead) and some are NFTs (arrow).

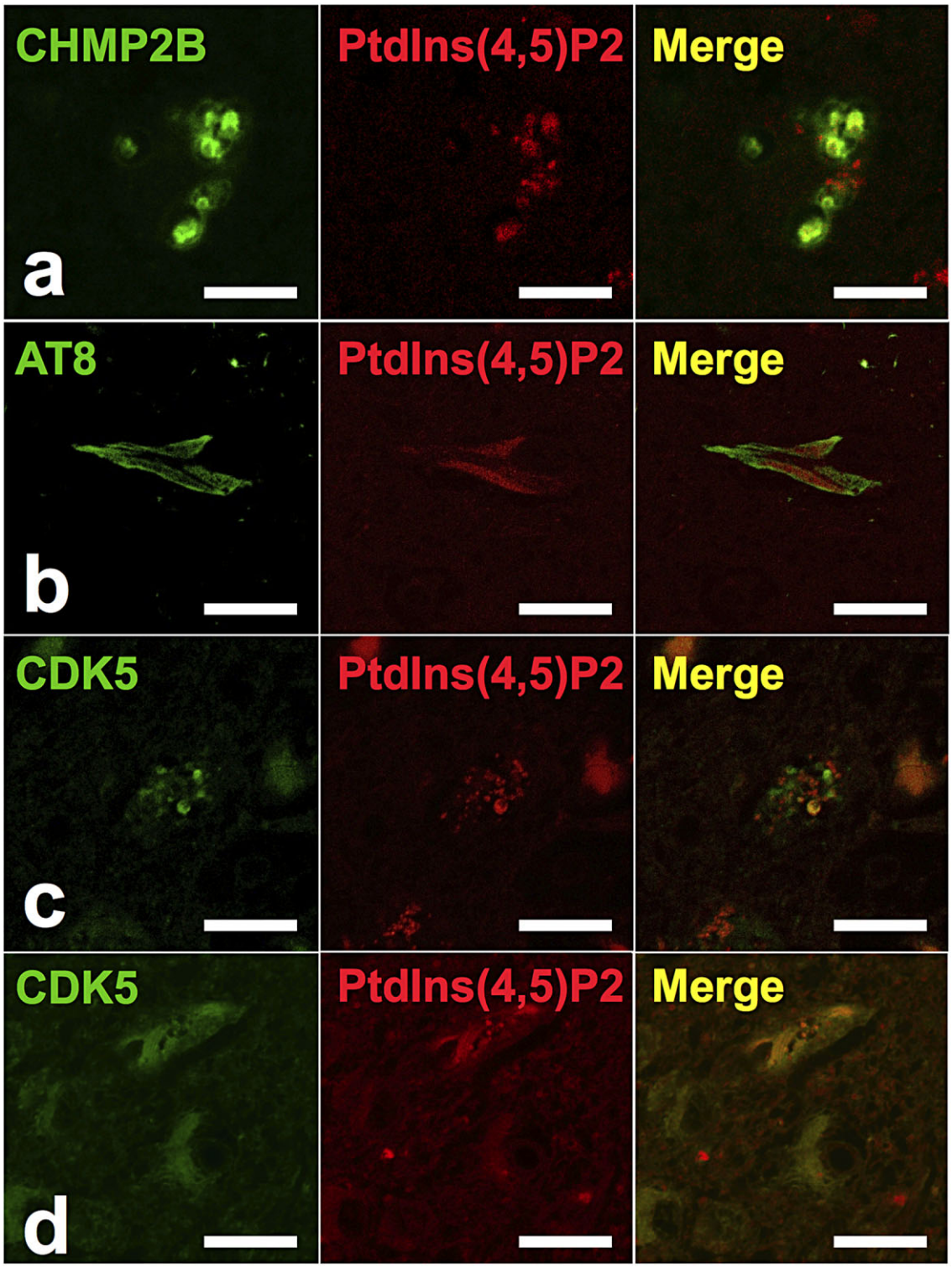

Figure 4. Representative confocal laser scanning micrograph. Double immunofluorescence labeling for (**a**) CHMP2B (green) and PtdIns(4,5)P2 (red), (**b**) AT8 (green) and PtdIns(4,5)P2 (red), (**c**,**d**) CDK5 (green) and PtdIns(4,5)P2 (red), (**e**,**f**) flotillin-1 (green) and PtdIns(4,5)P2 (red), and (**g**,**h**) annexin 2 (green) and PtdIns(4,5)P2 (red) and merged images in sections from patients with AD. For optimum visualization of the relationship, images from two channels were assigned the pseudocolour red [568 nm, for PtdIns(4,5)P2 in (**b**) and (**e**,**f**)] or green (488 nm, for AT8 and flotillin-1) and merged. Scale bars:10 μm.

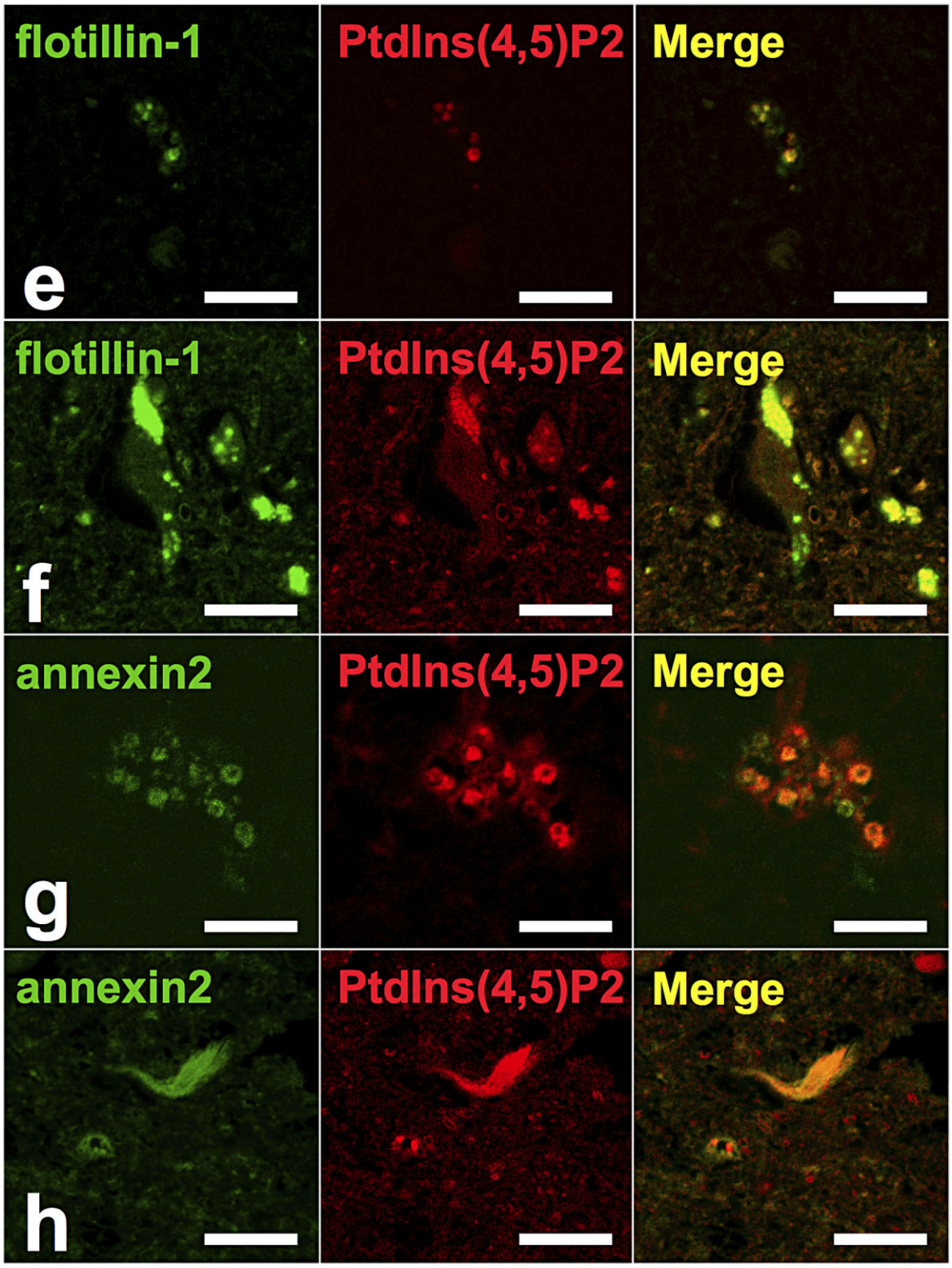

Figure 4. (*Continued*)

showed the same sensitivity for GVD bodies and NFTs. The lack of background staining suggests that the concentration of PtdIns(4,5)P2 in these structures is much higher than the physiological level. Thereby, from the standpoint of lipid composition, GVD bodies and NFTs are related to each other. Of note, whereas immunoreactivity for PtdIns(4,5)P2 was evident in NFTs, PtdIns(4,5)P2 was segregated from tau within NFTs. This result is consistent with the previous report that flotillin-1 was not colocalized with tau in tangle-bearing neurones. In addition, it is of interest that PtdIns(4,5)P2-positive granules can occasionally be observed within and outside NFTs.

Physiologically, PtdIns(4,5)P2 is enriched in plasma membranes and intra-nuclear structures, and is involved in a variety of cellular functions, such as the internalization of GPI-anchored proteins, pre-mRNA processing, and activation of inward rectifier potassium channels [26]; however, in the present experimental condition, none of these structures were detected. In contrast, pathological accumulation of PtdIns(4,5)P2 was observed in cultured cells from patients with Lowe syndrome, an X-linked disorder that affects eyes, neurones and kidneys (OMIM 309000) [27]. Interestingly, loss of the causative gene OCRL resulted in the appearance of PtdIns(4,5)P2-positive giant cytoplasmic vacuoles [28]. In accordance with the granules reported by Girardot *et al*., PtdIns(4,5)P2-positive granules were shown to contain lipid raft compartments based on the findings that flottilin-1 and annexin 2 colocalized with them. Colocalization of CDK5 on these granules is in agreement with recent evidence that CDK5 is recruited to lipid rafts upon stimulation [29]. Funk *et al*. reported that GVD bodies are located in the endocytic pathway leading to lysosomal degradation via multivesicular bodies [30]. Although, PtdIns(3)P and PtdIns(3,5)P2 clearly mark endosomal and/or multivesicular bodies, a relatively small amount of PtdIns(4,5)P2 was also shown to be present in endocytic vesicles. Collectively, the PtdIns(4,5)P2-positive structures observed in tauopathies may have some relationship to endosomes.

Because the phosphorylation status of PtdIns can be altered along the course of vesicle transport, the presence of the same PtdIns on vesicles does not readily imply that the origin of vesicles is unique. CK1δ and CK1ε are seen in GVD bodies but not in NFTs [17], suggesting that GVD bodies and NFTs arise from two independent pathological processes. It is unlikely that such highly concentrated pools of PtdIns(4,5)P2 are synthesized from different sources by chance; therefore, there might be a common mechanism by which PtdIns(4,5)P2 accumulates within GVD bodies and NFTs. Moreover, immunohistochemistry of the hippocampus using the MPM2 antibody that recognizes a set of phosphoproteins in mitotic cells also revealed common antigenicity of GVD bodies and NFTs in accordance with our results. Conversely, phosphorylated ribosomal protein S6 (pS6), a specific marker for stress granules in model systems, localized to GVD bodies in AD hippocampi [31]. This phenomenon was more common in neurones not containing NFTs, suggesting that GVD bodies might be a morphologic checkpoint between cell death and reversible cellular stress. The differential distribution of CK isoforms is likely analogous to the endosomal sorting complex required for transport (ESCRT) pathway in which a distinct set of subunits is recruited onto vesicles sequentially, and might be associated with neuronal viability.

In conclusion, our data indicate that PtdIns(4,5)P2 as well as lipid raft-associated proteins might equally affect the formation of GVD bodies and NFTs. Lipid raft-associated materials might have roles in all processes of degeneration in AD. Further investigation of the lipid composition of these granules will enable us to elucidate more precisely the pathological mechanisms underlying AD.

Acknowledgements

The authors would like to thank Ms Furuno, Ms Sasanishi and Ms Hironaka for their excellent technical assistance, and the Analysis Center of Life Science, Hiroshima University, Hiroshima, Japan, for the use of its facilities. This work was supported by grants from the Japanese Ministry of Education, Culture, Sports, Science, and Technology to M. Matsumoto, and in part by a grant from the Smoking Research Foundation, Tokyo, Japan to T. Takahashi.

Author contributions

Conceived and designed the experiments: T.N., T.T., M.N. and M.M. Performed the experiments: T.N., T.T. and M.N. Analysed the data: T.N., T.T. and M.N. Contributed reagents/materials/analysis tools: T.N., T.T., M.N., Y.Y., T.K., Y. Nagano, Y. Nishida and Y. I. Wrote the paper: T.N., T.T., M.N. and M.M.

Conflicts of interest

The authors state that they have no conflicts of interest to declare.

References

1 Kadokura A, Yamazaki T, Kakuda S, Makioka K, Lemere CA, Fujita Y, Takatama M, Okamoto K. Phosphorylation-dependent TDP-43 antibody detects intraneuronal dot-like structures showing morphological characters of granulovacuolar degeneration. *Neurosci Lett* 2009; **463**: 87–92

2 Baig S, van Helmond Z, Love S. Tau hyperphosphorylation affects Smad 2/3 translocation. *Neuroscience* 2009; **163**: 561–70

3 Yamazaki Y, Takahashi T, Hiji M, Kurashige T, Izumi Y, Yamawaki T, Matsumoto M. Immunopositivity for ESCRT-III subunit CHMP2B in granulovacuolar degeneration of neurons in the Alzheimer's disease hippocampus. *Neurosci Lett* 2010; **477**: 86–90

4 Leroy K, Boutajangout A, Authelet M, Woodgett JR, Anderton BH, Brion JP. The active form of glycogen synthase kinase-3beta is associated with granulovacuolar degeneration in neurons in Alzheimer's disease. *Acta Neuropathol* 2002; **103**: 91–9

5 Nakamori M, Takahashi T, Yamazaki Y, Kurashige T, Yamawaki T, Matsumoto M. Cyclin-dependent kinase 5 immunoreactivity for granulovacuolar degeneration. *Neuroreport* 2012; **23**: 867–72

6 Girardot N, Allinquant B, Langui D, Laquerriere A, Dubois B, Hauw JJ, Duyckaerts C. Accumulation of flotillin-1 in tangle-bearing neurones of Alzheimer's disease. *Neuropathol Appl Neurobiol* 2003; **29**: 451–61

7 Sui Z, Kovacs AD, Maggirwar SB. Recruitment of active glycogen synthase kinase-3 into neuronal lipid rafts. *Biochem Biophys Res Commun* 2006; **345**: 1643–8

8 Hernandez P, Lee G, Sjoberg M, Maccioni RB. Tau phosphorylation by cdk5 and Fyn in response to amyloid peptide Abeta (25-35): involvement of lipid rafts. *J Alzheimers Dis* 2009; **16**: 149–56

9 Rushworth JV, Hooper NM. Lipid rafts: linking Alzheimer's amyloid-beta production, aggregation, and toxicity at neuronal membranes. *Int J Alzheimers Dis* 2010; **2011**: 603052

10 Taylor DR, Hooper NM. Role of lipid rafts in the processing of the pathogenic prion and Alzheimer's amyloid-beta proteins. *Sem Cell Dev Biol* 2007; **18**: 638–48

11 Hooper NM. Roles of proteolysis and lipid rafts in the processing of the amyloid precursor protein and prion protein. *Biochem Soc Trans* 2005; **33**: 335–8

12 Cordy JM, Hooper NM, Turner AJ. The involvement of lipid rafts in Alzheimer's disease. *Mol Membr Biol* 2006; **23**: 111–22

13 Williamson R, Usardi A, Hanger DP, Anderton BH. Membrane-bound beta-amyloid oligomers are recruited into lipid rafts by a fyn-dependent mechanism. *FASEB J* 2008; **22**: 1552–9

14 Sobo K, Chevallier J, Parton RG, Gruenberg J, van der Goot FG. Diversity of raft-like domains in late endosomes. *PLoS ONE* 2007; **2**: e391

15 Golub T, Caroni P. PI(4,5)P2-dependent microdomain assemblies capture microtubules to promote and control leading edge motility. *J Cell Biol* 2005; **169**: 151–65

16 Roth MG. Phosphoinositides in constitutive membrane traffic. *Physiol Rev* 2004; **84**: 699–730

17 Thal DR, Del Tredici K, Ludolph AC, Hoozemans JJ, Rozemuller AJ, Braak H, Knippschild U. Stages of granulovacuolar degeneration: their relation to Alzheimer's disease and chronic stress response. *Acta Neuropathol* 2011; **122**: 577–89

18 Thal DR, Rüb U, Orantes M, Braak H. Phases of A beta-deposition in the human brain and its relevance for the development of AD. *Neurology* 2002; **58**: 1791–800

19 Braak H, Braak E. Neuropathological stageing of Alzheimer-related changes. *Acta Neuropathol* 1991; **82**: 239–59

20 Mirra SS, Heyman A, McKeel D, Sumi SM, Crain BJ, Brownlee LM, Vogel FS, Hughes JP, van Belle G, Berg L. The Consortium to Establish a Registry for Alzheimer's Disease (CERAD). Part II. Standardization of the neuropathologic assessment of Alzheimer's disease. *Neurology* 1991; **41**: 479–86

21 Hyman BT, Phelps CH, Beach TG, Bigio EH, Cairns NJ, Carrillo MC, Dickson DW, Duyckaerts C, Frosch MP, Masliah E, Mirra SS, Nelson PT, Schneider JA, Thal DR, Thies B, Trojanowski JQ, Vinters HV, Montine TJ. National Institute on Aging-Alzheimer's Association guidelines for the neuropathologic assessment of Alzheimer's disease. *Alzheimers Dement* 2012; **8**: 1–13

22 Watt SA, Kular G, Fleming IN, Downes CP, Lucocq JM. Subcellular localization of phosphatidylinositol 4,5-bisphosphate using the pleckstrin homology domain of phospholipase C delta1. *Biochem J* 2002; **363**: 657–66

23 Thomas CL, Steel J, Prestwich GD, Schiavo G. Generation of phosphatidylinositol-specific antibodies and their characterization. *Biochem Soc Trans* 1999; **27**: 648–52

24 Osborne SL, Thomas CL, Gschmeissner S, Schiavo G. Nuclear PtdIns(4,5)P2 assembles in a mitotically regulated particle involved in pre-mRNA splicing. *J Cell Sci* 2001; **114**: 2501–11

25 Hammond GR, Dove SK, Nicol A, Pinxteren JA, Zicha D, Schiavo G. Elimination of plasma membrane phosphatidylinositol (4,5)-bisphosphate is required for exocytosis from mast cells. *J Cell Sci* 2006; **119**: 2084–94

26 Huang CL, Feng S, Hilgemann DW. Direct activation of inward rectifier potassium channels by PIP2 and its stabilization by Gbetagamma. *Nature* 1998; **391**: 803–6

27 Kirkham M, Parton RG. Clathrin-independent endocytosis: new insights into caveolae and non-caveolar lipid raft carriers. *Biochim Biophys Acta* 2005; **1746**: 349–63

28 Zhang X, Hartz PA, Philip E, Racusen LC, Majerus PW. Cell lines from kidney proximal tubules of a patient with Lowe syndrome lack OCRL inositol polyphosphate

5-phosphatase and accumulate phosphatidylinositol 4,5-bisphosphate. *J Biol Chem* 1998; **273**: 1574–82

29 Ben El Kadhi K, Roubinet C, Solinet S, Emery G, Carreno S. The inositol 5-phosphatase dOCRL controls PI(4,5)P2 homeostasis and is necessary for cytokinesis. *Curr Biol* 2011; **21**: 1074–9

30 Funk KE, Mrak RE, Kuret J. Granulovacuolar degeneration (GVD) bodies of Alzheimer's disease (AD) resemble late-stage autophagic organelles. *Neuropathol Appl Neurobiol* 2011; **37**: 295–306

31 Castellani RJ, Gupta Y, Sheng B, Siedlak SL, Harris PLR, Coller JM, Perry G, Lee H, Tabaton M, Smith MA, Wang X, Zhu X. A novel origin for granulovacuolar degeneration in aging and Alzheimer's disease: parallels to stress granules. *Lab Invest* 2011; **91**: 1777–86

Received 27 September 2012
Accepted after revision 24 April 2013
Published online Article Accepted on 30 April 2013